

ScienceDirect



IFAC PapersOnLine 58-20 (2024) 392-397

Nonlinear control design for a spherical Wave Energy Converter.

Habeebullah Abdulkadir * Ossama Abdelkhalik * Mohamed A. Shabara *

* Department of Aerospace Engineering, Iowa State University, Ames, IA 50010, USA (e-mail: (see https://www.aere.iastate.edu/ossama/).

Abstract: This paper discusses the development of two nonlinear controls for a nonlinear spherical wave energy converter (WEC) to maximize the energy it harvests from the waves. The first control is a simple nonlinear damping control, which is designed based on the hydrodynamic damping coefficients. These control coefficients are then optimized using a Genetic Algorithm. The second is a nonlinear optimal control derived analytically using the Pontryagin minimum principle for comparison. The study found that the nonlinear optimal control improves the device's performance by effectively leveraging the hydrodynamic nonlinearity from the floater's shape. The nonlinear bang-singular-bang (BSB) control showed an average 20% performance improvement over the nonlinear damping control (NLDC).

Copyright © 2024 The Authors. This is an open access article under the CC BY-NC-ND license (https://creativecommons.org/licenses/by-nc-nd/4.0/)

Keywords: Wave energy converter, Control design, Optimal control, Nonlinear model, Nonlinear Froude-Krylov forces.

1. INTRODUCTION

Decarbonization has gained global attention in recent years with many countries seeking to reduce carbon dioxide emissions. Wind and solar sources are some of the popular renewable energy sources being harnessed; alongside these sources, ocean energy has great potential to be a major additional renewable energy source. However, for this to happen, the technology has to achieve a comparable energy cost. Several wave energy technologies have been developed over the years; one of the more popular types of Wave Energy Converters (WECs) is the point absorber (Brekken, 2011; Pastor and Liu, 2014).

A point absorber will generate the maximum power when its motion resonates with the exciting wave frequency. Controls seek to improve the energy extraction of the device when resonance is not achieved. While many control methods have been proposed over the years for WECs (Faedo et al., 2017; Abdulkadir and Abdelkhalik, 2022; Shabara et al., 2021; Hals et al., 2011; Zou et al., 2017; Wilson et al., 2016; Abdelkhalik and Abdulkadir, 2021), they often based on a linear model of the WEC dynamics. However, a more precise model will incorporate the nonlinearities that impact the device.

The nonlinearity considered in this work arises from the buoy shape not being a vertical cylinder near the water surface, leading to nonlinear hydrostatic and dynamic forces. In linear dynamics, hydrostatic and dynamic forces are calculated over a constant wetted area. However, with varying geometry at the water surface, the pressure must be integrated over the submerged surface instantaneously. To achieve computational efficiency, we adopt the closed-form algebraic formulation for approximating nonlinear Froude-Krylov (FK) forces developed in (Giorgi and Ringwood, 2017; Giorgi et al., 2021).

Nonlinearities in the WEC dynamic model can originate from various sources, including but not limited to buoy geometry, PTO, hydrodynamic nonlinearity, and more. Several works (Zou et al., 2023; Na et al., 2018; Abdelkhalik and Darani, 2018; Richter et al., 2012) have developed different formulations for controlling nonlinear WECs subject to these nonlinearities. Similar to the formulation proposed in Song et al. (2020), one of the nonlinear control formulations considered in this work assumes the form:

$$u = -\alpha B(\omega)\dot{z} - \beta B(\omega)\dot{z}^3 \tag{1}$$

where α and β are control coefficients to be optimized, $B(\omega)$ is the hydrodynamic damping force on the device, and \dot{z} is the heave velocity of the device. The first term in the control force formulation represents one type of nonlinear damping force, while the second term represents another type. The control coefficients are optimized to maximize the power extraction by the spherical device.

For performance comparison, an optimal nonlinear control is analytically derived using Pontryagin's Minimum Principle within the framework of optimal control theory. The controllers are then applied to the same device under identical wave conditions. The paper is organized as follows: Section II outlines a linear dynamic model for a simplified WEC device. The algebraic approximation for the nonlinear Froude-Krylov force is discussed in Section III. Section IV explores the nonlinear dynamics. Control formulations are addressed in Section V, followed by the presentation of simulation results in Section VI. The paper concludes with Section VII.

2. SOLO WEC DYNAMICS

A second-order mass-spring-damper system, as shown in fig. 1 is usually a good representation of a simple WEC.

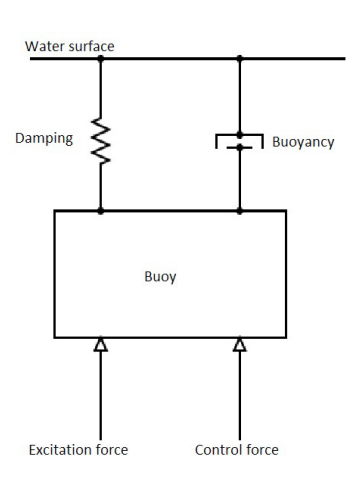


Fig. 1. Schematic of a simplified WEC device

Under the assumption of small wave height and motion amplitude, the motion of a floater, constrained to heave motion only, can be described using a linear equation of motion with one degree of freedom (1-DoF):

$$m\ddot{z} = f_e + f_r + f_s + u \tag{2}$$

where z is the heave displacement of the buoy from the sea surface, t is the time, m is the buoy mass, u is the control force, and $f_s = -Kz$ is the hydrostatic restoring force. f_e is the excitation force, f_r is the radiation force

3. NONLINEAR FROUDE-KRYLOV FORCE ALGEBRAIC APPROXIMATION.

For spherical geometry, as depicted in Fig. 2, the mean wetted surface changes instantaneously. Unlike in the linear model, where the excitation force comprises the hydrodynamic forces computed over a constant mean wetted surface area of the floater. The hydrostatic and hydrodynamic forces need to be computed at each time step for the nonlinear geometry. To mitigate the computational burden associated with using high-fidelity models to compute these forces, (Giorgi and Ringwood, 2017) developed an algebraic method for calculating nonlinear Froude-Krylov (FK) forces applicable to axisymmetric heaving point absorbers. The total Froude-Krylov (FK) force consists of the hydrostatic force FK_{st} and the dynamic force FK_{dy} . The nonlinear hydrostatic force represents the difference between the gravitational force \mathcal{F}_g and the static FK force on the buoy.

$$F_{FK} = F_g - \int_0^{2\pi} \int_{\sigma_1}^{\sigma_2} P(t) \mathbf{n} dS \tag{3}$$

The instantaneous pressure P(t) acts on the infinitesimal element ndS. According to Airy's wave theory, the total pressure for deep water waves is defined as:

$$P(t) = \rho g e^{\chi \sigma} \eta(t) \cos(\omega t) - \rho g \sigma(t) \tag{4}$$

where, g denotes gravitational acceleration, χ denotes wave number, ρ represents water density, $\eta(t)$ signifies free surface elevation, and ω indicates wave frequency. The magnitude of the heaving Froude-Krylov forces is given by:

$$F_{FK} = \int_0^{2\pi} \int_{\sigma_1}^{\sigma_2} P(t) f'(\sigma) f(\sigma) d\sigma d\theta \tag{5}$$

$$F_{FK}=\int_{0}^{2\pi}\int_{\sigma_{1}}^{\sigma_{2}}(\rho g e^{\chi\sigma}\eta(t)cos(\omega t)-\rho g\sigma(t))f'(\sigma)f(\sigma)d\sigma d\theta$$
 (6)

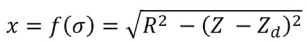
where h_0 represents the draft of the buoy at equilibrium, and $Z_d(t)$ denotes the instantaneous displacement of the buoy from its equilibrium position. The algebraic Froude-Krylov (FK) forces for the spherical and sloped line profiles depicted in Fig. 2 can be computed using the equations defined in Eq. (6). The free surface elevation and the draft of the buoy are the limit of integration based as:

$$\sigma_1 = -h_0 + Z_d(t) - \eta(t), \ \sigma_2 = 0$$
 (7)

For the spherical buoy, the nonlinear hydrostatic and hydrodynamic forces of can be computed as:

$$F_{FK_{static}} = F_g - 2\pi \rho g \left[\frac{(-R + Z_d - \eta(t))^3}{3} - \frac{(-R + Z_d - \eta(t))^2}{2} (Z_d + \eta(t)) \right] \quad \left(8 - \frac{1}{2} \right) = 0$$

$$F_{FK_{dynamic}} = -\frac{2\pi\rho g\eta(t)}{\chi}cos(\omega t)\left[\left(\sigma - Z_d + \eta(t) - \frac{1}{\chi}\right)e^{\chi\sigma}\right]_{\sigma_1}^{\sigma_2} \eqno(9)$$



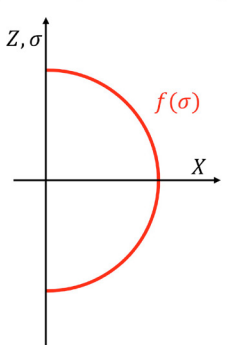


Fig. 2. Geometry of a spherical WEC device

4. NONLINEAR SOLO WEC DYNAMICS

The nonlinear equation of motion for a single-degree-of-freedom (1-DoF) WEC, considering heave motion only, is:

$$m\ddot{x}(t) = F_{NLFK} - u - \mu \ddot{x}(t) - c\dot{x} \tag{10}$$

$$F_{NLFK} = F_{FK_{dyn} + F_{FK_{ct}}} \tag{11}$$

$$M\ddot{x}(t) = F_{NLFK} - u - c\dot{x} \tag{12}$$

z is the buoy heave displacement, M is the total mass, control force u, and $F_{FK_{st}}$ is the static FK force and $F_{FK_{dyn}}$ is the dynamic FK force.

5. CONTROL FORMULATIONS

In this section, the two control methods considered are formulated; the first is the nonlinear control optimization approach, where the controller is optimized with the device design, and the second is the optimal control formulation based on the same devices. The device in consideration is a spherical WEC with a radius of 5m.

5.1 Nonlinear control optimization

In this study, the objective is to find the optimal coefficients of the nonlinear damping control formulation which maximize the power extraction of the considered nonlinear device. The optimization goal focuses on the time-averaged power output from the device:

$$J = \frac{1}{T} \int_{0}^{t_f} \{-u(t)x_2(t)\}dt$$

$$s.t. \ \alpha \in [\alpha_{min}. \ \alpha_{max}.],$$

$$\beta \in [\beta_{min}. \ \beta_{max}.].$$
(13)

As discussed in the introduction, the optimized nonlinear damping control coefficients will used in nonlinear control formulation:

$$u = -\alpha B(\omega)\dot{z} - \beta B(\omega)\dot{z}^3 \tag{14}$$

Table 1. Constraints on the optimization parameters.

Parameter	Unit	Lower Bound	Upper Bound
α	-	0.01	3
β	-	0.01	3

where α and β denote the control coefficients to be optimized, $B(\omega)$ represents the maximum hydrodynamic damping force on the device, and \dot{z} signifies the heave velocity of the device. The variable bounds are detailed in Table 1. Genetic Algorithm was used for the optimization. A flowchart illustrating the optimization setup is depicted in Fig. 3.

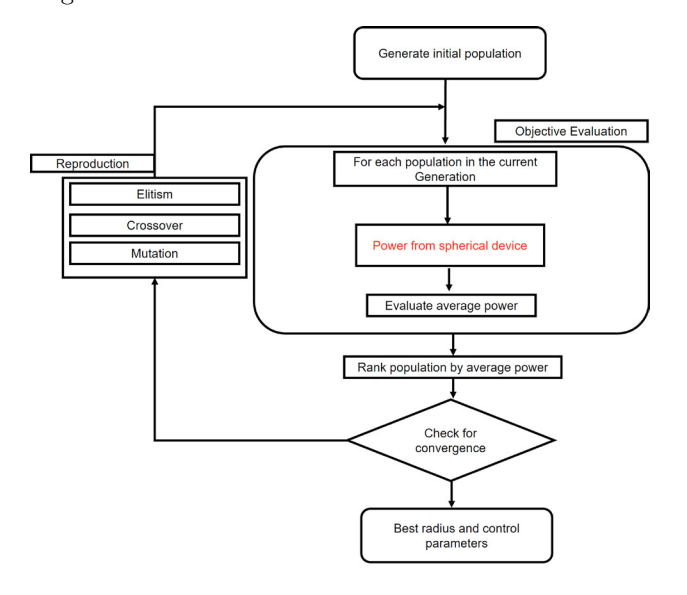


Fig. 3. GA flowchart for control co-design optimization.

5.2 Optimal control

In the context of a single WEC device, as considered in this paper, the objective function can be expressed as:

Min
$$J(u(t)) = \int_0^{t_f} \{-u(t)z_2(t)\}dt$$
 (15)

s.t. Eq. (12) and the control force constraint:

$$|u| \le U_{max} \tag{16}$$

This constraint Eq. (16) is on the PTO force, such that the force does not exceed the constraint at any time during the operation of the device. The Pontryagin's minimum principle (Pontryagin, 1987; Macki and Strauss, 2012) is used to solve the optimal control problem. If we define z_1 as the position of the floater and z_2 as its velocity, then the equation of motion for the system in fig. 1 can be rewritten in state space form as:

$$\dot{z}_1 = z_2 \tag{17}$$

$$\dot{z}_2 = \frac{1}{M} (F_{NLFK} - cz_2 - u) \tag{18}$$

where F_{NLFK} is nonlinear FK force, where the wave in this case is assumed a regular wave, and u is the control input. Based on the equations of motion of the buoy, we need to formulate the optimal control problem as follows:

$$Min: J((z(t), u(t))) = \int_0^{t_f} \{-u(t)z_2(t)\}dt$$
 (19)

Subject to: Eq. (17), and Eq. (18)

To start solving, we need to write out the Hamiltonian of the problem Bryson and Ho (2018):

$$H = -uz_2 + \lambda_1 z_2 + \frac{\lambda_2}{m} (F_{NLFK} - cz_2 - u)$$
 (20)

Based on the Hamiltonian, the necessary condition of the problem corresponding to $(z_1^*, z_2^*, u^*, \lambda_1^*, \lambda_2^*)$ which satisfy the Euler-Langrange equation is derived as:

$$H_{\lambda} = \dot{z} \tag{21}$$

$$H_z = -\dot{\lambda} \tag{22}$$

$$H_u = 0 (23)$$

By solving for the necessary conditions for optimality, we obtain the equations below and also the state space equation:

$$\dot{\lambda}_1 = -\frac{\lambda_2}{m} \frac{\partial F_{NLFK}}{\partial z_1} \tag{24}$$

$$\dot{\lambda}_2 = -\lambda_1 + \frac{c}{m}\lambda_2 + u \tag{25}$$

$$z_2 + \frac{\lambda_2}{m} = 0 \tag{26}$$

Since $H_u = 0$, the solution in Eq. (26) does not yield an expression for the control u, which means the control is either on a singular arc or at its boundaries (limits).

From Eq. (26),

$$\dot{z}_2 + \frac{\dot{\lambda}_2}{m} = 0 \tag{27}$$

combining Eq. (24) and Eq. (26),

$$\dot{\lambda}_1 = -\frac{\lambda_2}{m} \frac{\partial F_{NLFK}}{\partial z_1} \Rightarrow \frac{\partial F_{NLFK}}{\partial z_1} z_2 \Rightarrow \frac{\partial F_{NLFK}}{\partial z_1} \dot{z}_1 \quad (28)$$

Integrate Eq. (28)

$$\lambda_1 = \frac{\partial F_{NLFK}}{\partial z_1} z_1 + const. \tag{29}$$

$$\lambda_1 = F_{NLFK} + const. \tag{30}$$

Substitute Eq. (30) into Eq. (25)

$$\dot{\lambda}_2 = -F_{NLFK} - const. + \frac{c}{m}\lambda_2 + u \tag{31}$$

solving Eq. (18) for u and substituting in Eq. (31)

$$\dot{\lambda}_2 = -F_{NLFK} - const. + \frac{c}{m}\lambda_2 + [-m\dot{z}_2 - cz_2 + F_{NLFK}]$$
(32)

substituting Eq. (26) and Eq. (27) into Eq. (32) and simplifying

$$const = -2cz_2 \tag{33}$$

differentiating

$$0 = -2c\dot{z}_2\tag{34}$$

substitute for \dot{z}_2 from Eq. (18)

$$0 = -\frac{2c}{M}(F_{NLFK} - cz_2 - u) \tag{35}$$

Solving for u in Eq. (35), we can find the optimal control to be

$$u_{sa} = -cz_2 + F_{NLFK} \tag{36}$$

Substitute the optimal control u_{sa} from Eq. (36) into the system model in Eq. (18), and solving for the states, we get the switching condition as:

$$H_u = z_2 - \frac{2c}{M}(F_{NLFK} - cz_2)$$
 (37)

If there is a saturation on the control, and the buoy is subject to oscillatory excitation forces, then it is possible to state that the optimal control can be defined as:

$$u = \begin{cases} \Upsilon, H_u > 0 \\ u_{sa}, H_u = 0; \\ -\Upsilon, H_u < 0 \end{cases}$$

where Υ is the maximum available control level, and u_{sa} is the singular arc control.

6. SIMULATION RESULTS

The devices used in the simulation is a spherical single-body point absorber with a 5m radius. The controls developed in Section 5 are tested on the device in a regular wave environment with a period T=6 s and wave height H=0.8222 m. The simulation results for the optimized coefficients for the co-design controller (NLDC) tabulated

in Table 2 are compared with the nonlinear Bang-Singular-Bang (BSB) control. The hydrodynamic parameters (radiation damping and added mass) as functions of the frequency were obtained from NEMOH boundary element method (BEM) Matlab routine. The maximum control force availed by the PTO is $\Upsilon=5e6$ N.

Table 2. The optimized control parameters for the sphere

β
1.8493
1.9793
1.6143

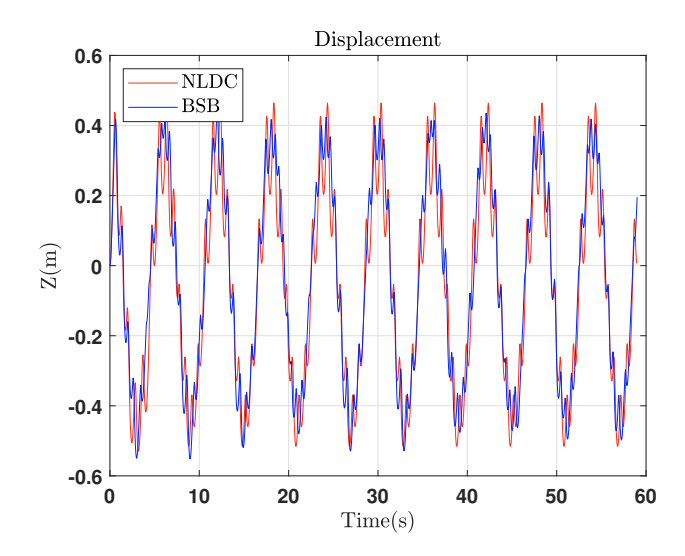


Fig. 4. Displacements when using NLDC and BSB.

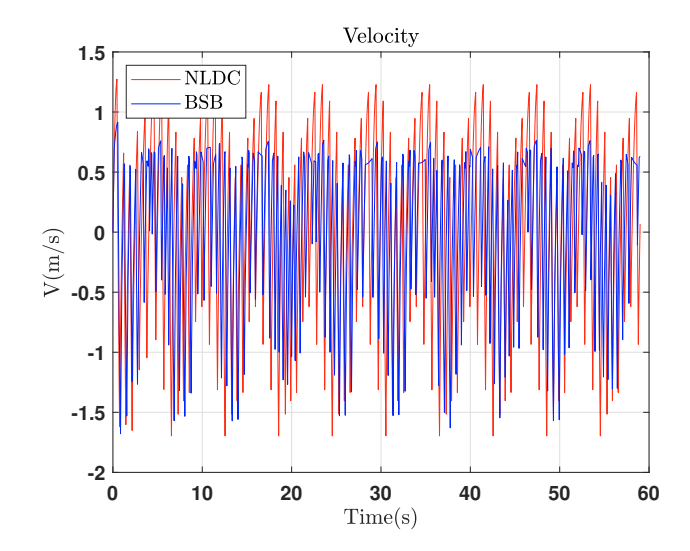


Fig. 5. Velocity when using NLDC and BSB.

The nonlinear motion of the device can be seen from the plot of its displacement plotted in Figure 4; it can be observed that the displacement when controlled using the NLDC control is close but slightly larger than when the BSB is used. Similarly, in Figure 5, the device's velocity when using BSB control is plotted against the velocity of the NLDC-controlled device.

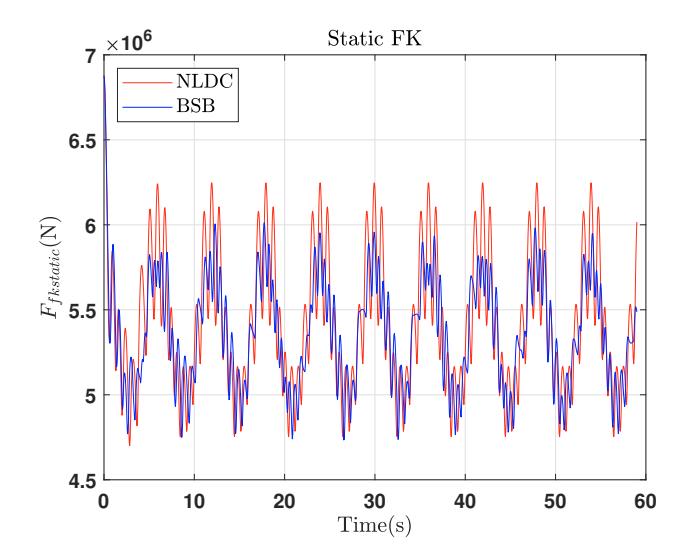


Fig. 6. Static FK forces when using NLDC and BSB.

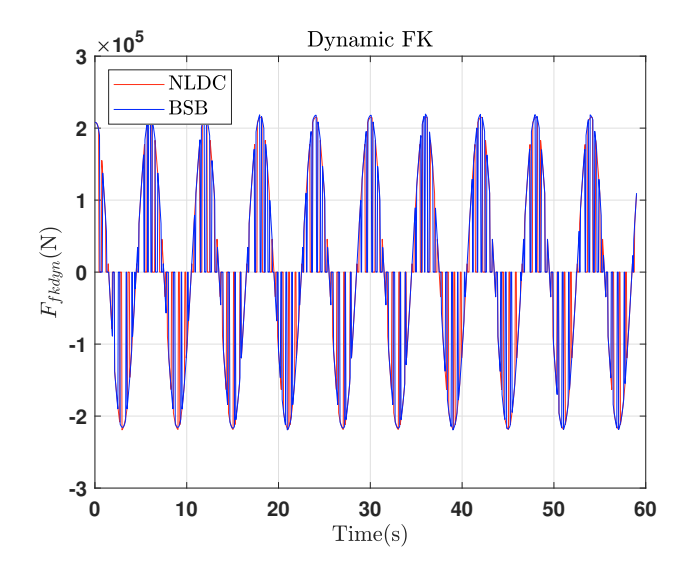


Fig. 7. Dynamic FK forces when using NLDC and BSB.

Figures. 6 and 7 show the static and dynamic FK forces acting on the buoy, respectively. On each figure, the magnitude of the forces acting on the device when using the control methods in consideration is plotted. Comparing the NLDC control and the BSB control, it is observed that while the static FK force is of higher magnitude for the NLDC control, the dynamic FK forces are comparable for both controllers, with the dynamic FK force being zero when the motion of the device grow to be too large.

In the BSB control formulation, it shows that the solution of the optimal control will be on the singular arch when the switching condition presented in Eq. (37) is zero. However, the condition is small but not zero at all times; in this case, the bound for the singular arc condition will be set to $abs(H_u) < 0.01$. Figure 8 shows the resulting control forces generated using each control method. The magnitude of forces generated is contained to be within the limits. The power plot from both controls is plotted in figure 9, it can be observed that the BSB has some power curve going below the zero line; this is the reactive power requirement of the control method. Overall, a 20.65% energy improvement was recorded for the BSB over the NLDC

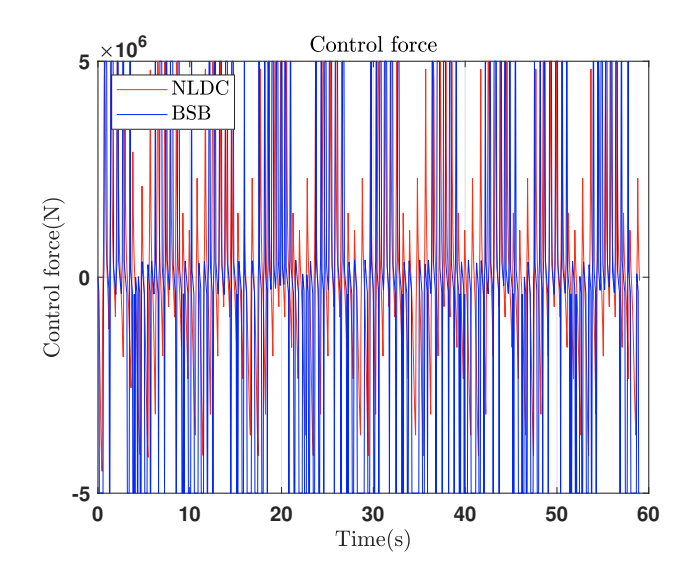


Fig. 8. PTO forces when using NLDC and BSB.

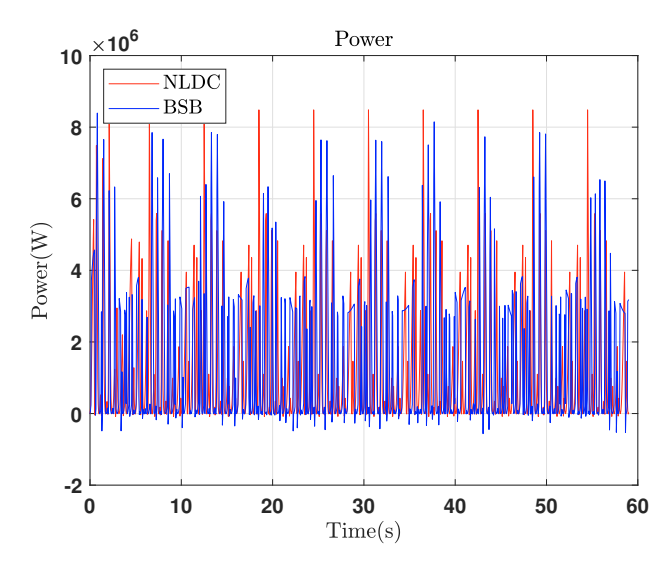


Fig. 9. Power when using NLDC and BSB.

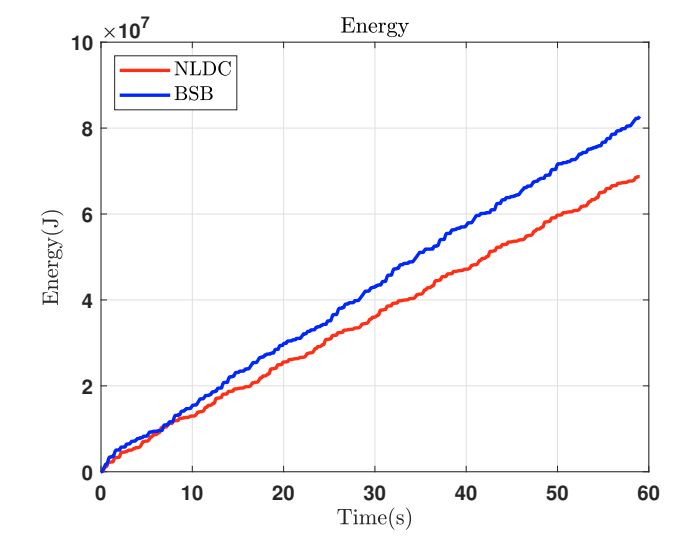


Fig. 10. Energy when using NLDC and BSB.

control as presented in figure 10. In all simulations, the BSB outperformed the optimal NLDC control formulation.

7. CONCLUSION

Two nonlinear control formulations were presented to control a spherical nonlinear WEC. The goal is to maximize the power output from wave energy converters with strong nonlinear Froude-Krylov (FK) forces. The FK forces were derived algebraically; a nonlinear damping control was formulated and optimized while accounting for the nonlinearity in the system. For comparison, an optimal nonlinear control formulation was derived analytically within the context of optimal control theory. Simulation results presented in this paper show that the overall performance of the optimal Bang-singular-bang control obtained from the analytical derivation approach achieved significantly higher power output than that of the nonlinear damping control (NLDC), which was optimized using genetic algorithm. The wave considered in this current work is monochromatic. Future work will develop and test the performance of the control approaches for devices experiencing irregular excitation.

ACKNOWLEDGEMENTS

This paper is based upon work supported by NSF, Grant Number 2048413. The research reported in this paper is partially supported by the HPC@ISU equipment at Iowa State University, some of which has been purchased through funding provided by NSF under MRI grant number 1726447.

REFERENCES

- Abdelkhalik, O. and Abdulkadir, H. (2021). Optimal control of wave energy converters. In OCEANS 2021: San Diego Porto, 1–5. doi: 10.23919/OCEANS44145.2021.9705961.
- Abdelkhalik, O. and Darani, S. (2018). Optimization of nonlinear wave energy converters. *Ocean Engineering*, 162, 187–195.
- Abdulkadir, H. and Abdelkhalik, O. (2022). Optimal constrained control of wave energy converter arrays. In 2022 American Control Conference (ACC), 3100–3105. doi:10.23919/ACC53348.2022.9867173.
- Brekken, T.K. (2011). On model predictive control for a point absorber wave energy converter. In 2011 IEEE Trondheim PowerTech, 1–8. IEEE.
- Bryson, A.E. and Ho, Y.C. (2018). Applied optimal control: optimization, estimation, and control. Routledge.
- Faedo, N., Olaya, S., and Ringwood, J.V. (2017). Optimal control, mpc and mpc-like algorithms for wave energy systems: An overview. *IFAC Journal of Systems and Control*, 1, 37–56.
- Giorgi, G. and Ringwood, J.V. (2017). Computationally efficient nonlinear froude–krylov force calculations for heaving axisymmetric wave energy point absorbers. *Journal of Ocean Engineering and Marine Energy*, 3, 21–33.
- Giorgi, G., Sirigu, S., Bonfanti, M., Bracco, G., and Mattiazzo, G. (2021). Fast nonlinear froude–krylov force calculation for prismatic floating platforms: a wave energy conversion application case. *Journal of Ocean Engineering and Marine Energy*, 7(4), 439–457.
- Hals, J., Falnes, J., and Moan, T. (2011). Constrained optimal control of a heaving buoy wave-energy converter.

- Journal of Offshore Mechanics and Arctic Engineering, 133(1).
- Macki, J. and Strauss, A. (2012). Introduction to optimal control theory. Springer Science & Business Media.
- Na, J., Wang, B., Li, G., Zhan, S., and He, W. (2018). Nonlinear constrained optimal control of wave energy converters with adaptive dynamic programming. *IEEE Transactions on Industrial Electronics*, 66(10), 7904–7915.
- Pastor, J. and Liu, Y. (2014). Frequency and time domain modeling and power output for a heaving point absorber wave energy converter. *International Journal of Energy and Environmental Engineering*, 5(2), 1–13.
- Pontryagin, L.S. (1987). Mathematical theory of optimal processes. CRC press.
- Richter, M., Magana, M.E., Sawodny, O., and Brekken, T.K. (2012). Nonlinear model predictive control of a point absorber wave energy converter. *IEEE Transactions on Sustainable Energy*, 4(1), 118–126.
- Shabara, M.A., Zou, S., and Abdelkhalik, O. (2021). Numerical investigation of a variable-shape buoy wave energy converter. In *International Conference on Off-shore Mechanics and Arctic Engineering*, volume 85192, V009T09A013. American Society of Mechanical Engineers.
- Song, J., Abdelkhalik, O., and Zou, S. (2020). Genetic optimization of shape and control of non-linear wave energy converters. In *International Conference on Off*shore Mechanics and Arctic Engineering, volume 84416, V009T09A036. American Society of Mechanical Engineers
- Wilson, D., Bacelli, G., Coe, R.G., Bull, D.L., Abdelkhalik, O., Korde, U.A., and Robinett III, R.D. (2016). A comparison of wec control strategies. Sandia National Laboratories Tech. Rep. SAND2016-4293, 10, 1431291.
- Zou, S., Abdelkhalik, O., Robinett, R., Bacelli, G., and Wilson, D. (2017). Optimal control of wave energy converters. *Renewable energy*, 103, 217–225.
- Zou, S., Song, J., and Abdelkhalik, O. (2023). A sliding mode control for wave energy converters in presence of unknown noise and nonlinearities. *Renewable Energy*, 202, 432–441.